Inventory of Supplemental Information

1. Extended Data Figures 1 - 7
2. Source Data Figures

Source Data Figures	Parental Figures	Legend
Source Data Fig. 1	Figure 3j/Extended Data Figures 5m	Images of Oil-Red-O lipid staining in SGBS adipocytes following lentiviral COBLL1 and GRB14 knock-down.
Source Data Fig. 2	Figure 3n	Western blots for lipolysis-relevant proteins assayed in basal or isoproterenol/IBMX stimulated differentiated shCOBLL1 compared to shEV SGBS adipocytes
Source Data Fig. 3	Extended Data Figure 5i, first row left	Microscopy images of COBLL1 antibody (green), actin (Phalloidin, red) and nuclei (Hoechst, blue) staining in siCOBLL1 and siNT visceral adipocytes.
Source Data Fig. 4	Extended Data Figure 5i, first row right	
Source Data Fig. 5	Extended Data Figure 5i, second row left	
Source Data Fig. 6	Extended Data Figure 5i, second row right	
Source Data Fig. 7	Extended Data Figure 5i, third row left	
Source Data Fig. 8	Extended Data Figure 5i, third row right	
Source Data Fig. 9	Extended Data Figure 5i, fourth row left	
Source Data Fig. 10	Extended Data Figure 5i, fourth row right	

Extended Data Figures

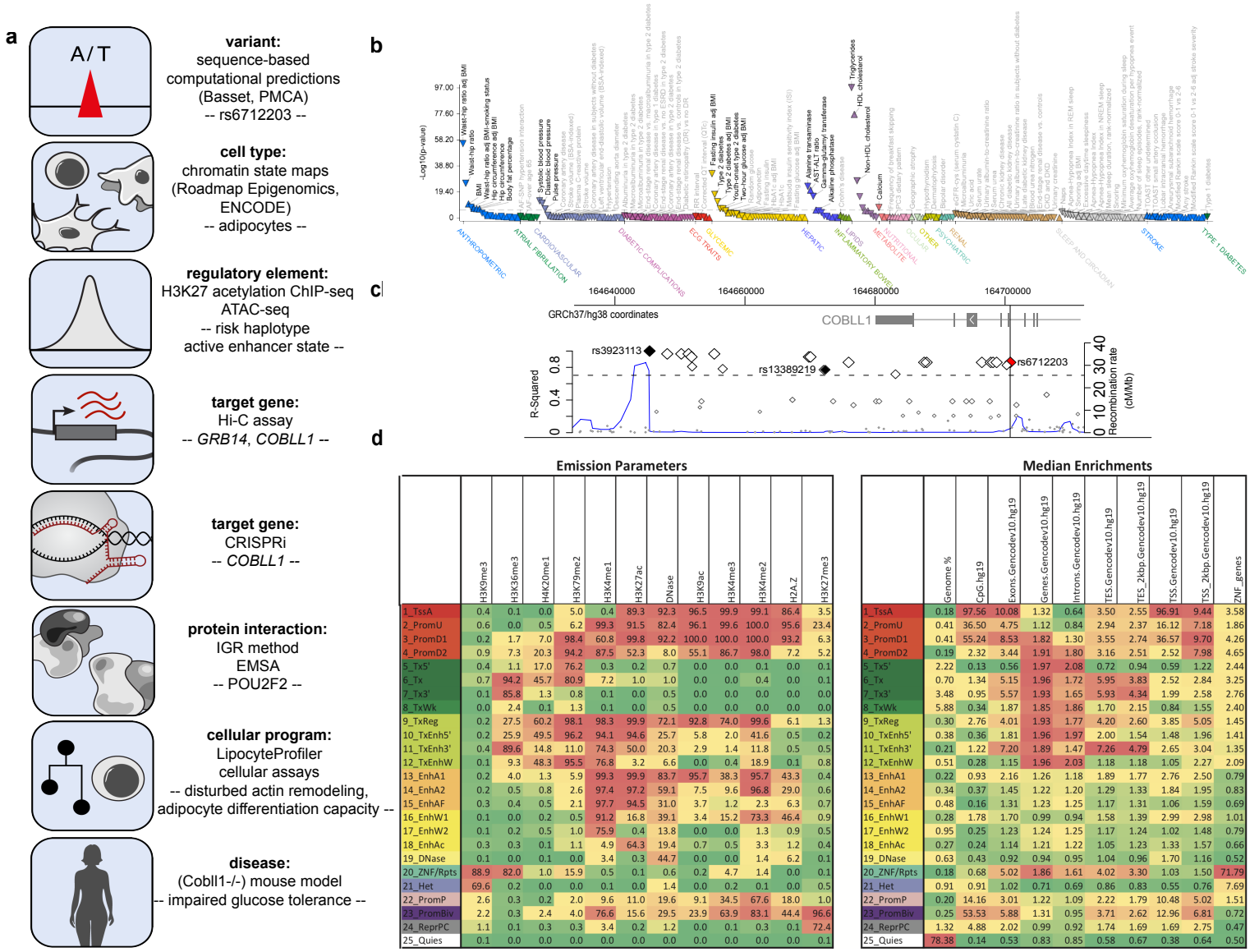

	H3K9me3	H3K36me3	H4K20me1	H3K79me2	H3K4me1	H3K27ac	DNase	H3K9ac	H3K4me3	H3K4me2	H2A.Z	H3K27me3
1_TssA	0.4	0.1	0.0	5.0	0.4	89.3	92.3	96.5	99.9	99.1	86.4	3.5
2_PromU	0.6	0.0	0.5	6.2	99.3	91.5	82.4	96.1	99.6	100.0	95.6	23.4
3_PromD1	0.2	1.7	7.0	98.4	60.8	99.8	92.2	100.0	100.0	100.0	93.2	6.3
4_PromD2	0.9	7.3	20.3	94.2	87.5	52.3	8.0	55.1	86.7	98.0	7.2	5.2
5_Tx5'	0.4	1.1	17.0	76.2	0.3	0.2	0.7	0.0	0.0	0.1	0.0	0.1
6_Tx	0.7	94.2	45.7	80.9	7.2	1.0	1.0	0.0	0.0	0.4	0.0	0.1
7_Tx3'	0.1	85.8	1.3	0.8	0.1	0.0	0.5	0.0	0.0	0.0	0.0	0.0
8_TxWk	0.0	2.4	0.1	1.3	0.1	0.0	0.5	0.0	0.0	0.0	0.0	0.0
9_TxReg	0.2	27.5	60.2	98.1	98.3	99.9	72.1	92.8	74.0	99.6	6.1	1.3
10_TxEnh5'	0.2	25.9	49.5	96.2	94.1	94.6	25.7	5.8	2.0	41.6	0.5	0.2
11_TxEnh3'	0.4	89.6	14.8	11.0	74.3	50.0	20.3	2.9	1.4	11.8	0.5	0.5
12_TxEnhW	0.1	9.3	48.3	95.5	76.8	3.2	6.6	0.0	0.4	18.9	0.1	0.8
13_EnhA1	0.2	4.0	1.3	5.9	99.3	99.9	83.7	95.7	38.3	95.7	43.3	0.4
14_EnhA2	0.2	0.5	0.8	2.6	97.4	97.2	59.1	7.5	9.6	96.8	29.0	0.6
15_EnhAF	0.3	0.4	0.5	2.1	97.7	94.5	31.0	3.7	1.2	2.3	6.3	0.7
16_EnhW1	0.1	0.0	0.2	0.5	91.2	16.8	39.1	3.4	15.2	73.3	46.4	0.9
17_EnhW2	0.1	0.2	0.5	1.0	75.9	0.4	13.8	0.0	0.0	1.3	0.9	0.5
18_EnhAc	0.3	0.3	0.1	1.1	4.9	64.3	19.4	0.7	0.5	3.3	1.2	0.4
19_DNase	0.1	0.0	0.1	0.0	3.4	0.3	44.7	0.0	0.0	1.4	6.2	0.1
20_ZNF/Rpts	88.9	82.0	1.0	15.9	0.5	0.1	0.6	0.2	4.7	1.4	0.0	0.1
21_Het	69.6	0.2	0.0	0.0	0.1	0.0	1.4	0.0	0.2	0.1	0.0	0.5
22_PromP	2.6	0.3	0.2	2.0	9.6	11.0	19.6	9.1	34.5	67.6	18.0	1.0
23_PromBiv	2.2	0.3	2.4	4.0	76.6	15.6	29.5	23.9	63.9	83.1	44.4	96.6
24_ReprPC	1.1	0.1	0.3	0.3	3.4	0.2	1.2	0.0	0.1	0.3	0.1	72.4
25_Quies	0.1	0.0	0.0	0.0	0.0	0.0	0.0	0.0	0.0	0.0	0.0	0.1

	Genome %	CpG.hg19	Exons.Gencodev10.hg19	Genes.Gencodev10.hg19	Introns.Gencodev10.hg19	TES.Gencodev10.hg19	TES_2kbp.Gencodev10.hg19	TSS.Gencodev10.hg19	TSS_2kbp.Gencodev10.hg19	ZNF_genes
1_TssA	0.18	97.56	10.08	1.32	0.64	3.50	2.55	96.91	9.44	3.58
2_PromU	0.41	36.50	4.75	1.12	0.84	2.94	2.37	16.12	7.18	1.86
3_PromD1	0.41	55.24	8.53	1.82	1.30	3.55	2.74	36.57	9.70	4.26
4_PromD2	0.19	2.32	3.44	1.91	1.80	3.16	2.51	2.52	7.98	4.65
5_Tx5'	2.22	0.13	0.56	1.97	2.08	0.72	0.94	0.59	1.22	2.44
6_Tx	0.70	1.34	5.15	1.96	1.72	5.95	3.83	2.52	2.84	3.25
7_Tx3'	3.48	0.95	5.57	1.93	1.65	5.93	4.34	1.99	2.58	2.76
8_TxWk	5.88	0.34	1.87	1.85	1.86	1.70	2.15	0.84	1.55	2.40
9_TxReg	0.30	2.76	4.01	1.93	1.77	4.20	2.60	3.85	5.05	1.45
10_TxEnh5'	0.38	0.36	1.81	1.96	1.97	2.00	1.54	1.48	1.96	1.41
11_TxEnh3'	0.21	1.22	7.20	1.89	1.47	7.26	4.79	2.65	3.04	1.35
12_TxEnhW	0.51	0.28	1.15	1.96	2.03	1.18	1.18	1.05	2.27	2.09
13_EnhA1	0.22	0.93	2.16	1.26	1.18	1.89	1.77	2.76	2.50	0.79
14_EnhA2	0.34	0.37	1.45	1.22	1.20	1.29	1.33	1.84	1.95	0.83
15_EnhAF	0.48	0.16	1.31	1.23	1.25	1.17	1.31	1.06	1.59	0.69
16_EnhW1	0.28	1.78	1.70	0.99	0.94	1.58	1.39	2.99	2.98	1.01
17_EnhW2	0.95	0.25	1.23	1.24	1.25	1.17	1.24	1.02	1.48	0.79
18_EnhAc	0.27	0.24	1.14	1.21	1.22	1.05	1.23	1.33	1.57	0.66
19_DNase	0.63	0.43	0.92	0.94	0.95	1.04	0.96	1.70	1.16	0.52
20_ZNF/Rpts	0.18	0.68	5.02	1.86	1.61	4.02	3.30	1.03	1.50	71.79
21_Het	0.91	0.91	1.02	0.71	0.69	0.86	0.83	0.55	0.76	7.69
22_PromP	0.20	14.16	3.01	1.22	1.09	2.22	1.79	10.48	5.02	1.51
23_PromBiv	0.25	53.53	5.88	1.31	0.95	3.71	2.62	12.96	6.81	0.72
24_ReprPC	1.32	4.88	2.02	0.99	0.92	1.74	1.69	1.69	2.75	0.47
25_Quies	78.38	0.14	0.53	0.83	0.85	0.58	0.67	0.38	0.64	0.50

Extended Data Figure 1

Extended Data Fig. 1. a) Schematic overview for the 2q24.3 metabolic risk locus dissection. Aim of step (top, bold); methods/experiments used (middle); key finding/result of each step (bottom). b) PheWAS of trait associations at the rs3923113-tagged haplotype of a meta-analysis https://t2d.hugeamp.org/. Colors represent trait classes while individual rs3923113 variant association p-values are shown on the Y axis. Direction of effect is indicated by orientation of triangles, upward: increase, downward: decrease c) The *2q24.3* MONW locus spans 19 non-coding SNPs in high linkage disequilibrium with rs3923113 (LD r2>0.8). The region of association localizes to a >55kb interval in an intergenic region between *COBLL1* and *GRB14*. d) Annotation panel and color key for the twenty-five state chromatin model70. Rows represent chromatin states abbreviations, columns are emission parameters, corresponding to the frequency with which each mark is expected in each state (left table) and genome coverage and median enrichments of relevant genomic annotations (right panel). TssA: Active TSS, TssAFlnk: Flanking Active TSS, TxFlnk: Transcription at gene 5' and 3', Tx: Strong Transcription, TxWk: Weak Transcription, EnhG: Genic enhancers: Enh: Enhancers, ZNF/Rpts: ZNF genes & repeats, Het: Heterochromatin, TssBiv: Bivalent/Poised TSS, BivFlnk: Flanking Bivalent TSS/Enhancer, EnhBiv: Bivalent Enhancer, ReprPC: Repressed Polycomb, ReprPCWk: Weak Repressed Polycomb, Quies: Quiescent/Low. e) Stranded allele-specific chromatin accessibility measures at the haplotype using ATAC-seq data in differentiating adipocytes from a heterozygous individual. For each day of differentiation of an individual heterozygous, the number of reads overlapping with 20 non-coding SNPs in the haplotype, ordered by their start position and strand relative to the position of the variant, are shown. More reads indicate higher activity in haplotype 1 (non-risk, blue) compared to haplotype 2 (risk yellow). x-axis: offset from SNP position (bp), y-axis: stranded read count. f) Replication of the effect at time 0 (mesenchymal stem cells) with ATAC-seq. g) BMI-dependent variant association analysis. Bar plots represent the beta of the rs6712203 association with type 2 diabetes following BMI stratification. The cohort analysed is the UK Biobank self-identified white British individuals (total N = 327,960; N = 109198 with BMI < 25, N = 140539 with BMI between 25 and 30, and N = 78223 with BMI >= 30), and overlay of data points is not practical. Betas and 95% confidence intervals are shown, derived from a two-sided generalized linear model on outcome adjusted for demographic covariates (age, sex, genotyping array, 40 PCs).

a

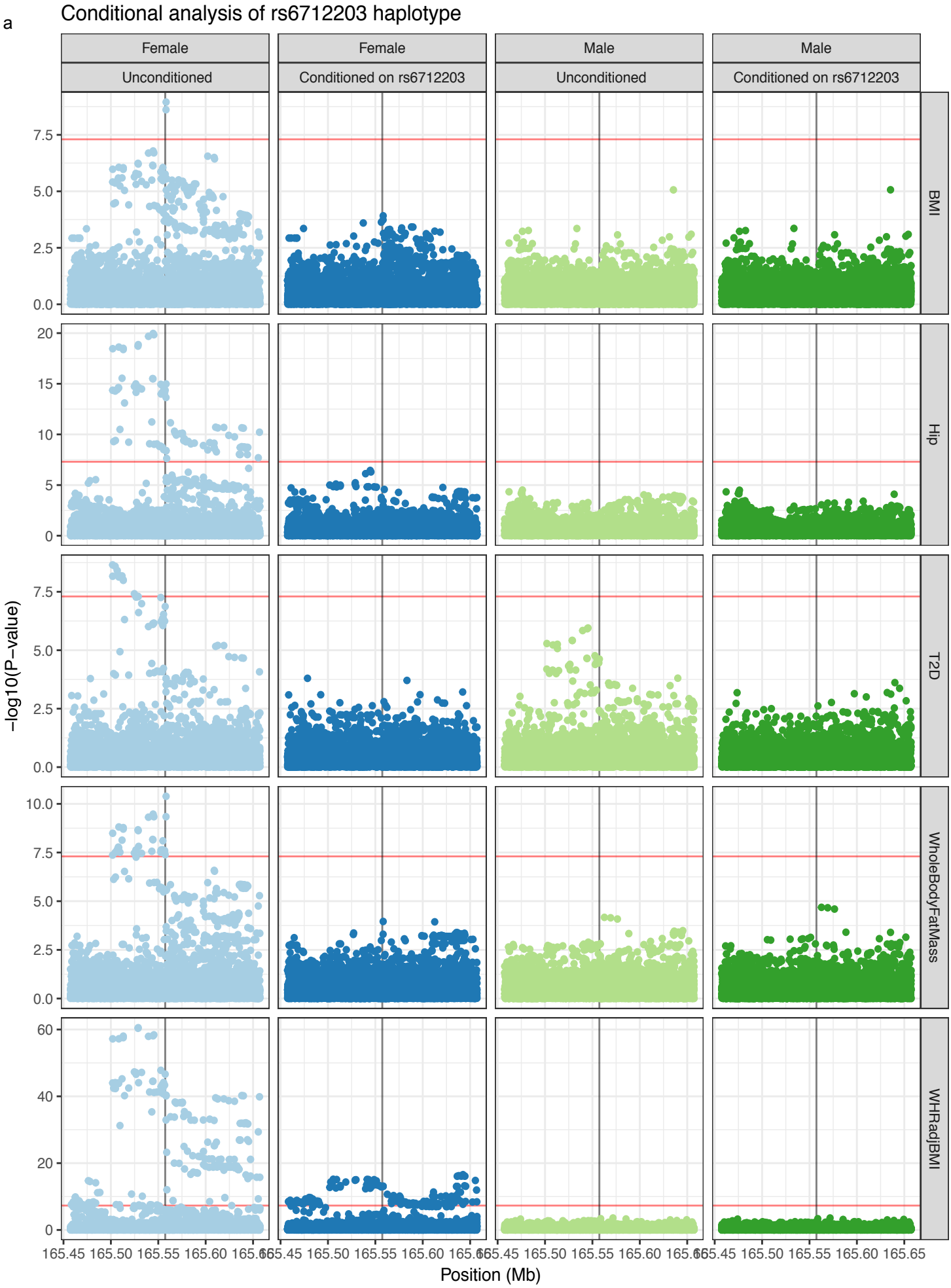

Extended Data Figure 2

Extended Data Fig. 2. Conditional analyses implicating rs6712203 in the genetic control of anthropometric traits and type 2 diabetes. Each panel represents a different trait / sex / conditional analysis window, and all panels have an X axis corresponding to 100kb on either side of the rs6712203 variant. The Y axis shows, for each variant in the window, the association strength for the given trait conditioned on the variants noted in White British participants in UK Biobank with the sex shown, and red lines indicate the significance threshold 5 x 10-8). -log10 p-values are shown, derived from a two-sided generalized linear model on outcome adjusted for demographic covariates (age, sex, genotyping array, 40 pcs).

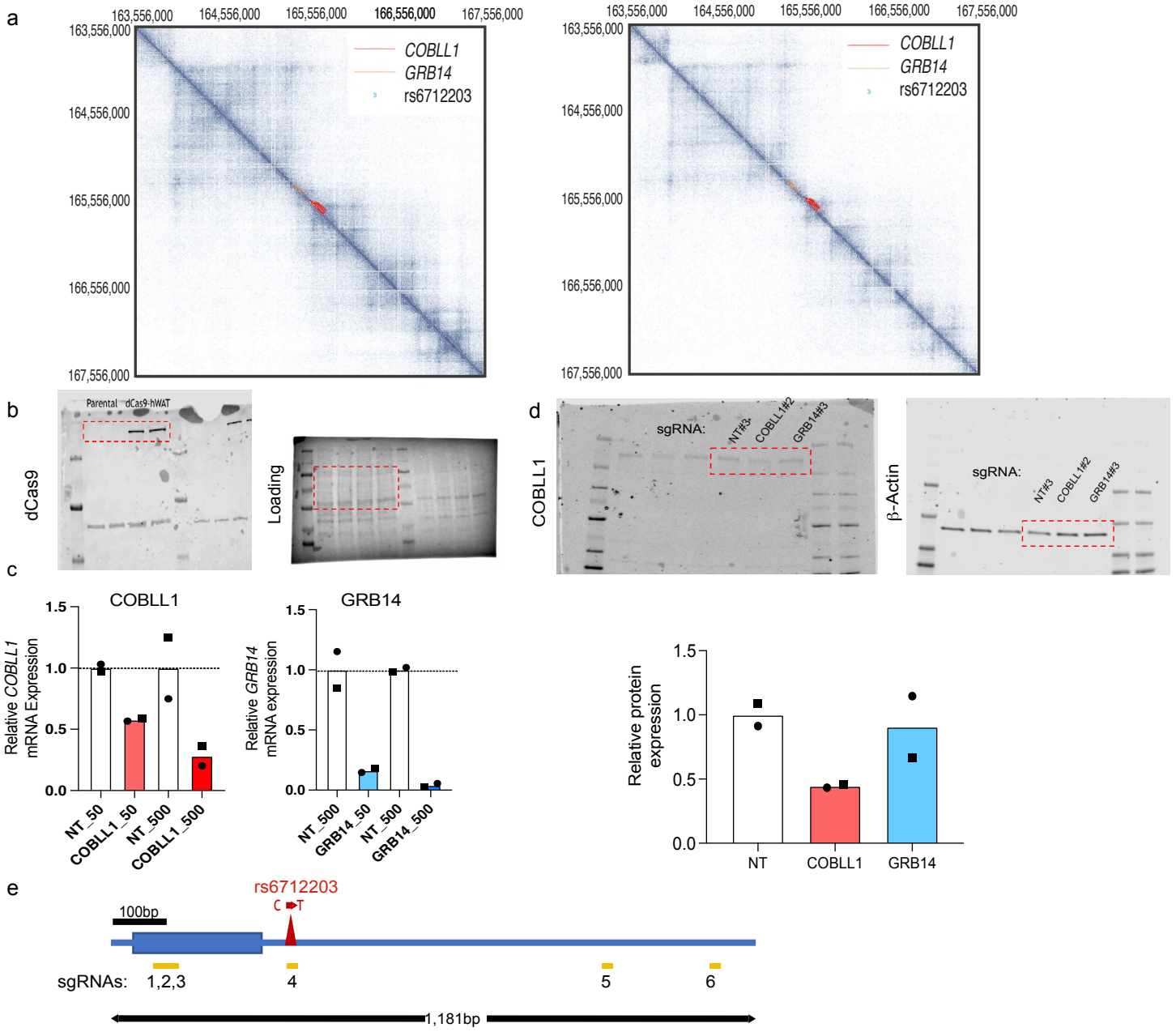

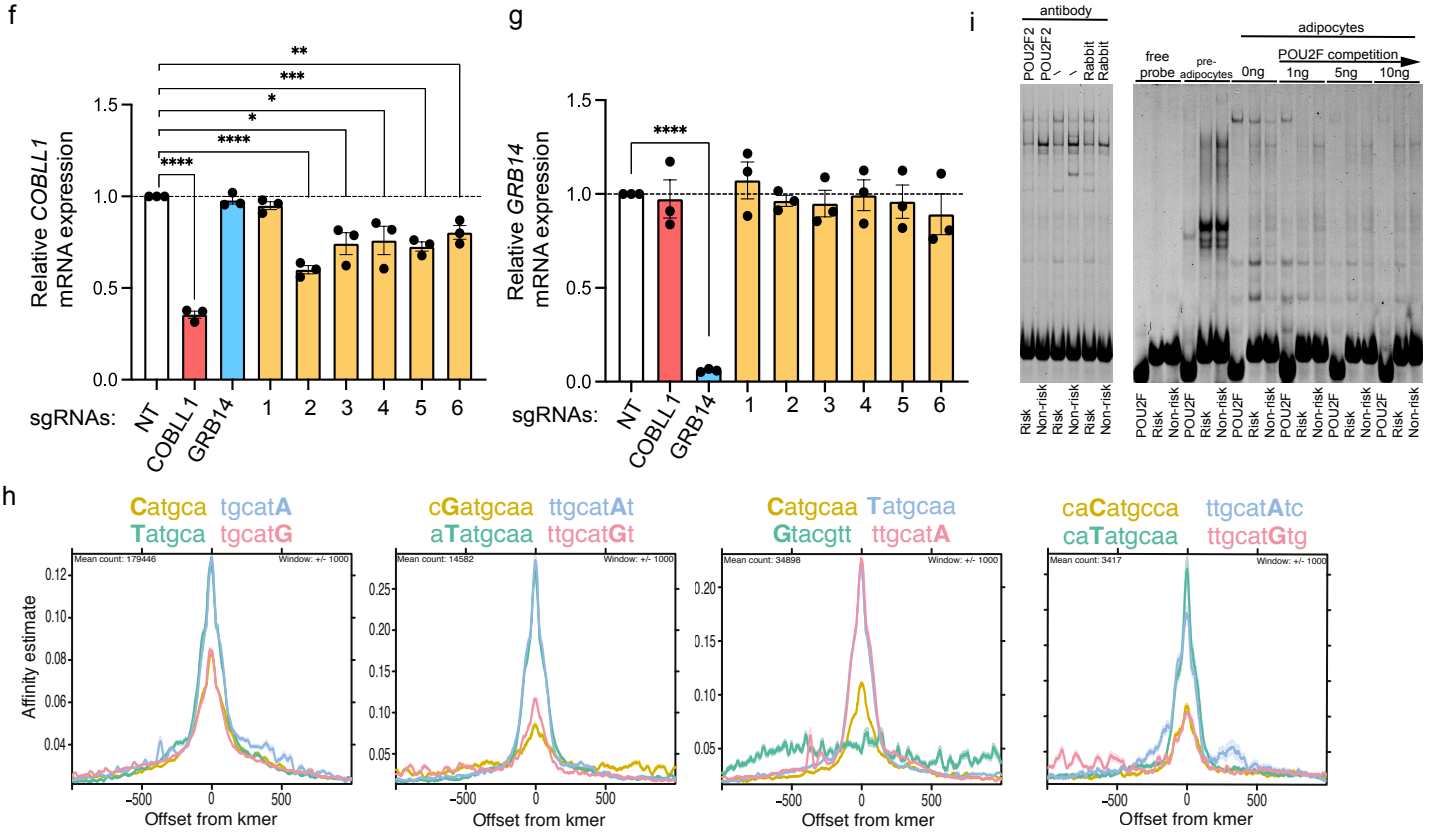

Extended Data Figure 3

Extended Data Fig. 3. a) Cross-cell type conserved genome-wide higher order chromatin interactions for the 2q24.3 locus analyzed by Hi-C assays in human fibroblasts (left) and NHEK primary normal human epidermal keratinocytes (right), chr2: 163,556,000 - 167,558,000 (hg19), binned at 2kb resolution. b) Cas9 protein expression in dCas9 hWAT compared to the parental hWAT cell line. c) mRNA expression of COBLL1 and GRB14 in response to increasing amounts of lentiviral sgRNA vectors (2 sgRNAs, virus volume 50 µl and 500 µl) targeting TSS regions of each gene compared to non-targeting controls (NT, 2 sgRNAs). Columns are means of individual sgRNAs indicated by different symbols. d) COBLL1 protein expression normalized to b-actin in dCas9 hWATs transduced with sgRNAs targeting COBLL1 or GRB14 compared to controls. Top panel: Image of gel of representative sgRNA targeting NT, COBLL1 or GRB14. Bottom panel: plot of protein expression; 2 sgRNA for each target in 2 replicates. e) Representation of 1,181bp region flanking the COBLL1 intronic variant rs6712203 at the 2q24.3 MONW locus showing individual sgRNAs (n=6) targeting the rs6712203 flanking regulatory region used in the CRISPRi experiments. f-g) mRNA expression of f) COBLL1 and g) GRB14 in undifferentiated dCas9-hWAT preadipocytes at 6 days post lentiviral transduction with sgRNAs targeting TSS regions (red: COBLL1 TSS; blue GRB14 TSS) and the rs6712203-flanking regulatory element at position 1 to 6 as depicted in e). Data are mean +/- SEM of 3 independent experiments. **** $P < 0.0001$, *** $P = 0.0004$, ** $P = 0.006$, * $P = 0.013 – 0.036$, two-tailed Student's *t* test. h) Predicted binding of POU2F2 between the two alleles using the Intragenomic Replicate Method (Cowper-Sal lari et al. 2012). As in Figure 2d with different kmer counts.

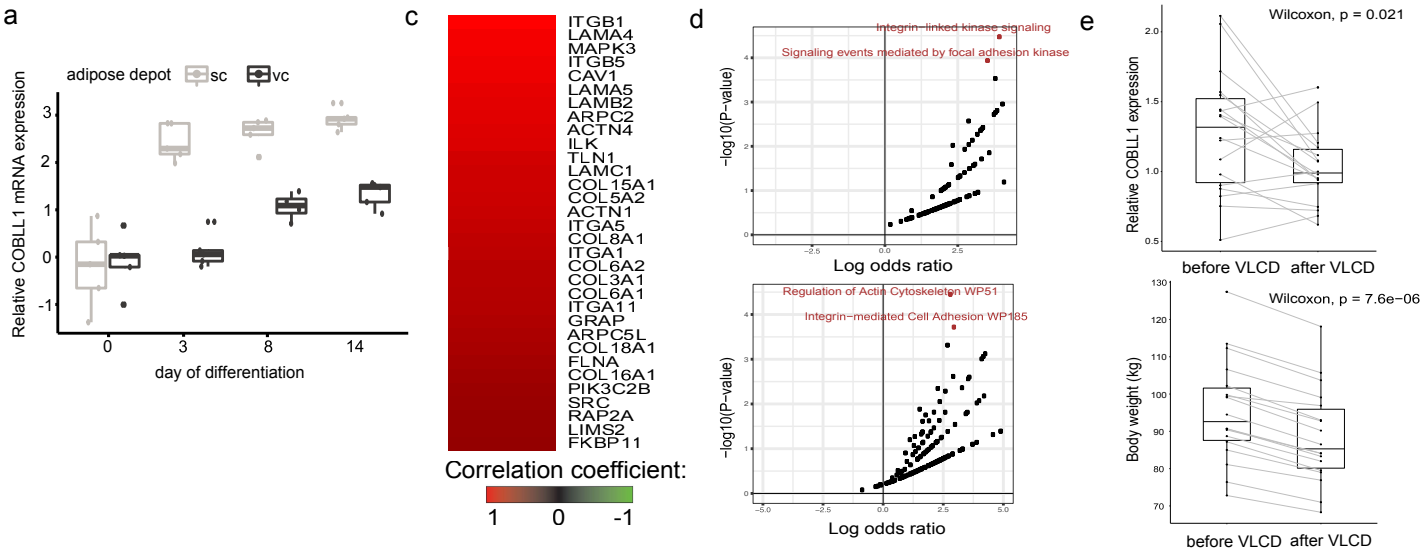

b

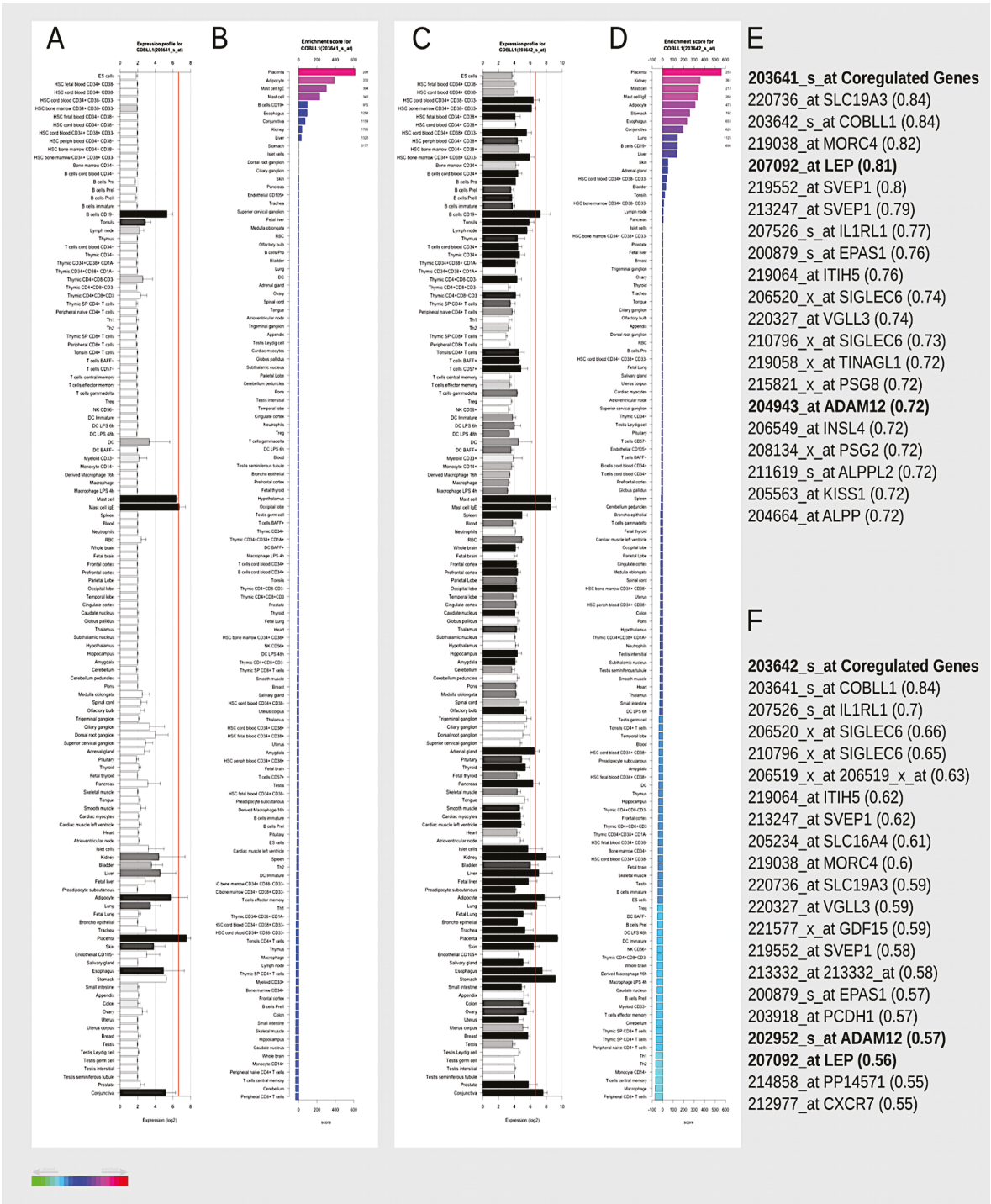

Extended Data Figure 4

Extended Data Fig. 4. a) COBLL1 expression in subcutaneous and visceral AMSCs throughout adipogenic differentiation, N=4 biologically independent experiments, t-test two-sided, data represent median + 95% CI. b) COBLL1 gene expression enrichment across 142 tissues (A-D) from enrichment profiler36. COBLL1 probes 203641_s_at and 203642_s_at were used for coregulation analysis (E-F). c) Correlation with COBLL1 probe ILMN_1761260 using microarray data from lean and individuals with obesity. d) Enrichment of pathways in the HCI (upper panel) and WikiPathways (lower panel) gene set lists from Enrichr, plotted as in Figure 3A (KEGG), with p-value thresholds corresponding to the FDR cutoffs in those data. p-values are derived from a hypergeometric test. e) COBLL1 expression in subcutaneous adipose tissue before and after a very low caloric diet (VLCD, upper panel, n=18), corresponding body weight (lower panel), Wilcoxon signed-rank test.

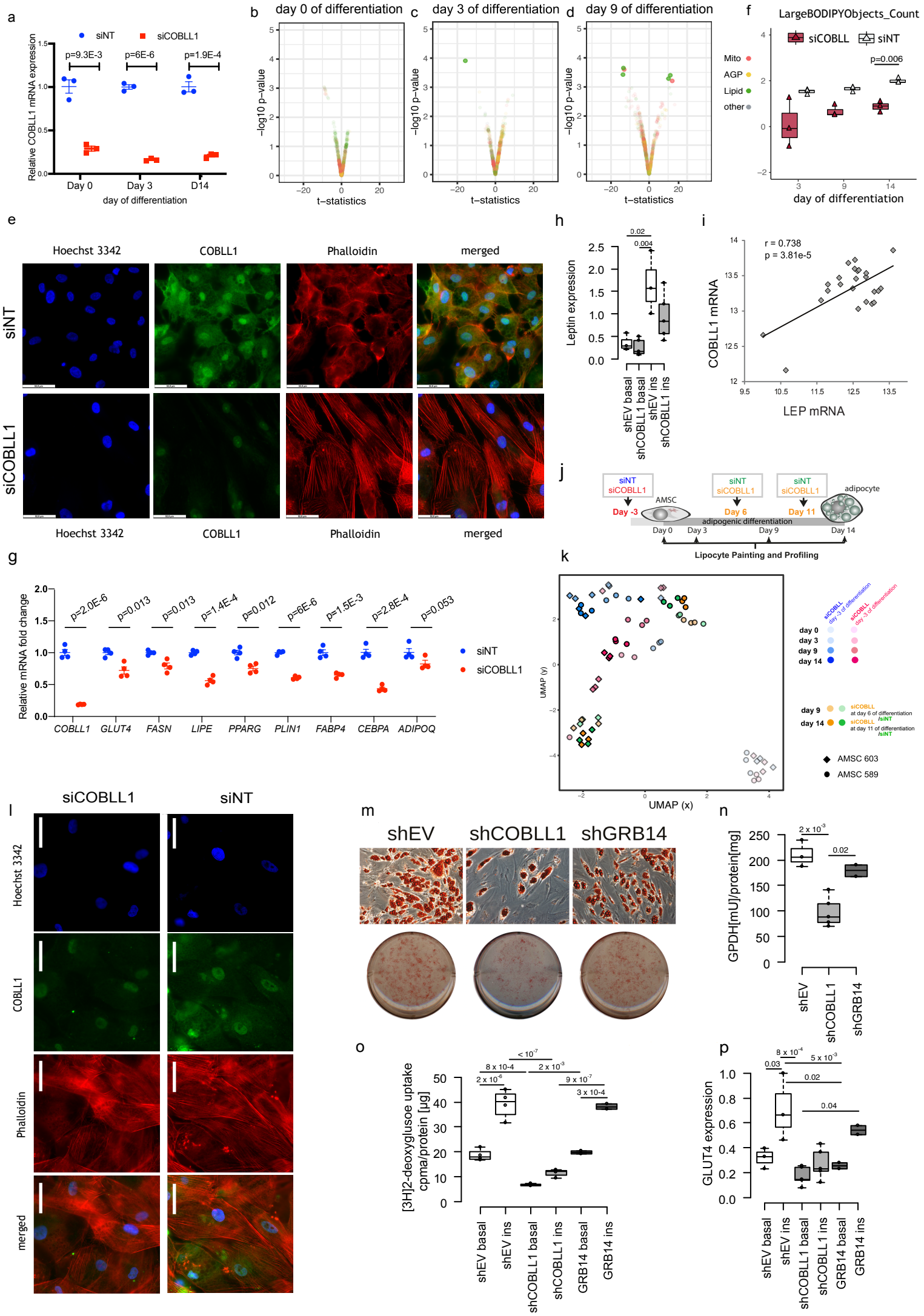

Extended Data Figure 5

Extended Data Fig. 5. a) COBLL1 expression in siCOBLL1 and siNT at day 0, 3 and 14 of differentiation, N=3 biologically independent experiments, t-test two-sided. knock-down efficiency 80%, mean values + SEM. b-d) Morphological profiles of siCOBLL compared to siNT AMSCs at day 0 (b) day 3 (c) and day 9 (d) of differentiation, t-test two-sided, significance level < 5% FDR. e) Actin and COBLL1 staining in siCOBLL1 compared to siNT subcutaneous adipocytes at day 9 using phalloidin and COBLL1 antibody staining (HPA053344, Alexa-Fluor 488), magnification x63/oil. Scale bar = 52.8 um. Representative results from N=3 independent experiments. f) Cells_Children_LargeBODIPY_objects_count in siCOBLL1- and siNT AMSCs at day 3, 9, 14, N=3 biologically independent experiments, t-test two-sided, significance level < 5% FDR. G) qPCR-based gene expression of COBLL1 and adipocyte marker genes GLUT4, FASN, LIPE, PPARG, PLIN1, FABP4, CEBPA, ADIPOQ in siCOBLL1 and siNT AMSCs at day 14 of differentiation, t-test two-sided, N=4 biologically independent experiments, mean values +/- SEM. h) qPCR-based leptin gene expression in shCOBLL1 compared to shEV adipocytes. Data are represented as median + 95% CI, one-way ANOVA with Tukey's HSD test, N=4 biologically independent experiments i) Correlation of COBLL1 mRNA with LEP mRNA in subcutaneous adipose tissue from 24 lean individuals measured by Illumina microarrays. The pearson's correlation coefficient r and p-value are depicted j) Schematic of siCOBLL1 KD and AMSCs differentiation. k) UMAP-based dimensionality reduction of LipocyteProfiler features in siCOBLL1 and siNT AMSCs. l) Actin and COBLL1 staining in siCOBLL1 and siNT visceral adipocytes at day 14 using phalloidin and COBLL1 antibody staining (HPA053344, Alexa-Fluor 488), magnification x63/oil. Representative result from N=2 independent experiments, scale bar = 52,8um m) Representative Oil-Red-O lipid staining in SGBS adipocytes following lentiviral *COBLL1* knock-down (shCOBLL1, knock-down efficiency 69%) and GRB14 (shGRB14, knock-down efficiency 61%) compared to empty vector control (shEV), scale bar = 15mm. n) GPDH metabolic activity in shCOBLL1, shGRB14 and shEV SGBS adipocytes, one-way ANOVA with Tukey's HSD test, mean + 95% CI, N=4 biologically independent experiments o) Basal and insulin-stimulated 3H-2-deoxyglucose uptake in shCOBLL1, shGRB14 and shEV SGBS adipocytes, one-way ANOVA with Tukey's HSD test, mean + 95% CI, N=4 biologically independent experiments, 1st and 3rd quartiles (box) and median (middle line) are indicated, $p=4.3 \times 10^{-8}$. p) qPCR-based *GLUT4* gene expression in shCOBLL1, shGRB14 and shEV adipocytes, one-way ANOVA with Tukey's HSD test, mean + 95% CI, N=4 biologically independent experiments.

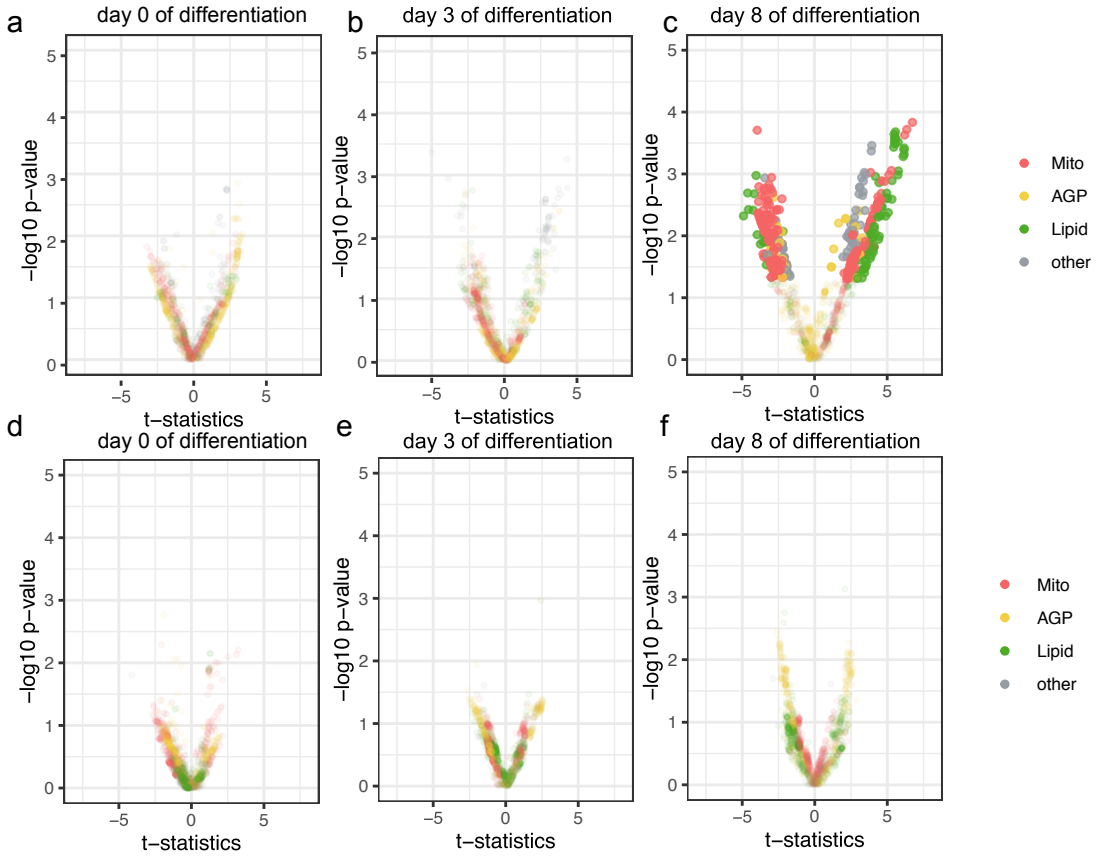

Extended Data Figure 6

Extended Data Fig. 6 a-c) Differences in morphological profiles between TT (n=7) and CC (n=6) allele carriers at day 0 (a), day 3 (b) and day 8 (c) in subcutaneous AMSCs (multi-way ANOVA, significance level < 5% FDR). d-f) Differences in morphological profiles between TT (n=7) and CC (n=6) allele carriers at (d) day 0, (e) day 3 and (f) day 8 in visceral AMSCs (multi-way ANOVA, significance level < 5% FDR).

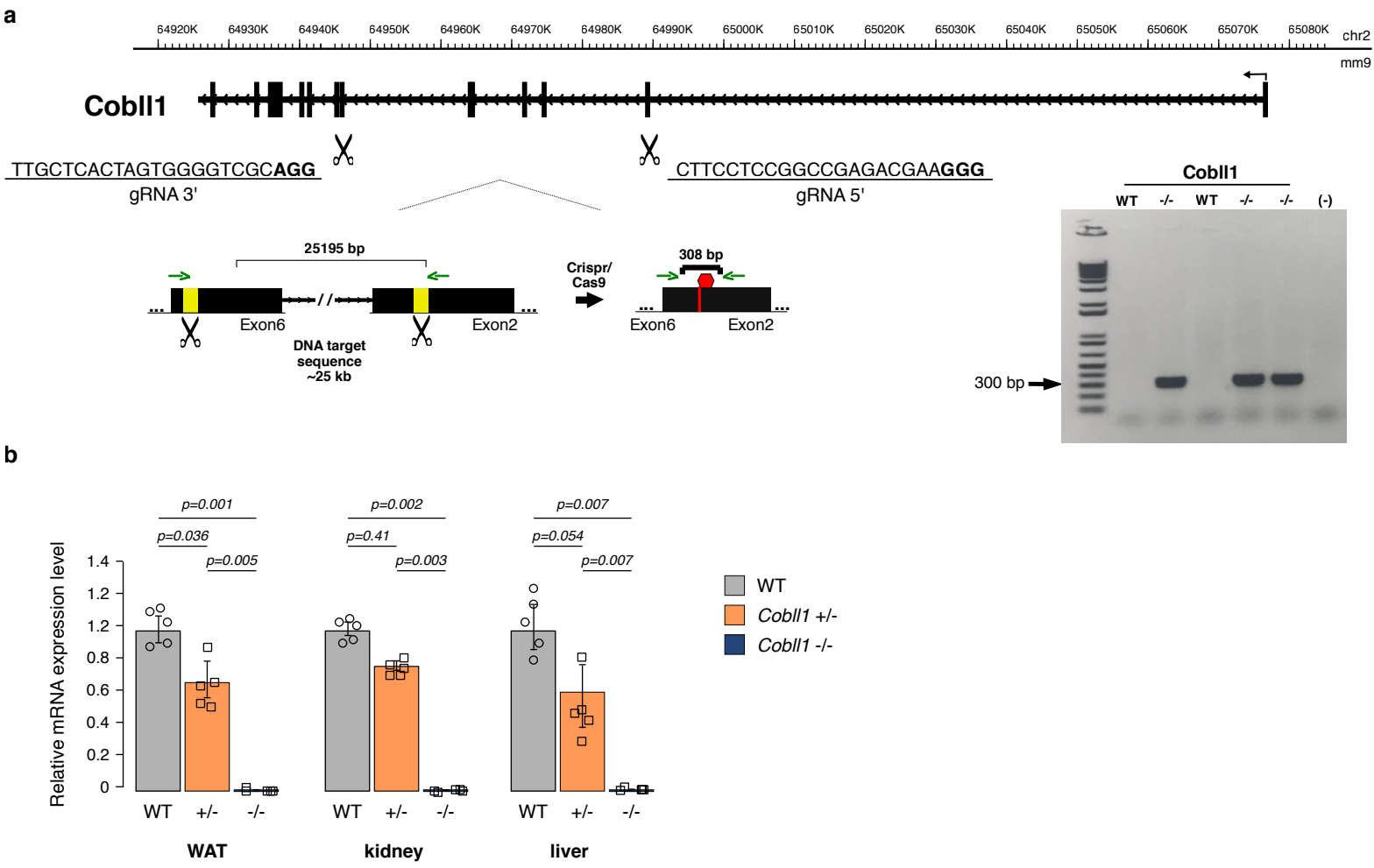

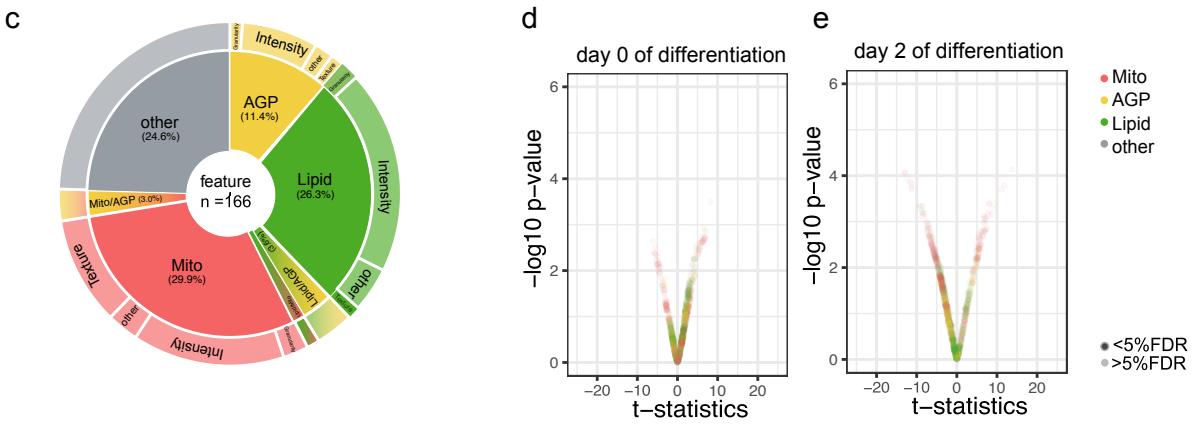

Extended Data Figure 7

Extended Data Fig. 7. Generation of Cobll1 mutant mice using CRISPR/Cas9 editing. a) Overview of the CRISPR/-Cas9 strategy to delete ~20 kb of the Cobll1 gene. The gRNA-targeting sequences (gRNAs) are underlined, and the PAM sequences are indicated in bold. Exons are represented as thick black boxes, introns are indicated as black lines with arrows, and the yellow boxes indicate the DNA-targeting region. Red hexagon indicates a stop codon generating a Cobll1 truncated protein. Agarose gel showing the PCR products generated from DNA containing successfully targeted Cobll1 from F0 mouse tail genomic DNA. The 308 bp band corresponds to the genomic deletion. b) A real-time quantitative PCR of levels of Cobll1 mRNA in white adipose tissue (WAT), liver and kidney of Cobll1 WT, Cobll1 heterozygous (+/-) and null knockout Cobll1 (-/-) animals to confirm the Cobll1 ablation in knockout animals. Each group was analyzed using 5 different mice and the values were expressed as the mean ± s.e.m and P values by Student's t-test. experiment was repeated independently two times with similar results. c) Pie chart illustrating non-redundant differential features per channel and class of measurement at day 8 of subcutaneous adipocyte differentiation in rs6712003 homozygous risk compared to non-risk carriers. d-e) Differences in morphological profiles between AMSCs from Cobll1-/- mice (n=3) and WT (n=4) at (h) day 0 (i) day 2 (t-test two-sided, significance level < 5%FDR).

Source Data Figures

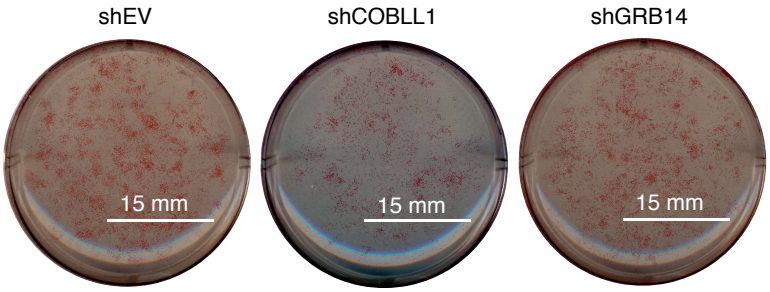

Source Data Fig. 1

Precision Plus Protein Dual Color standards

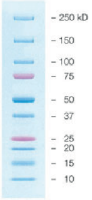

Bio-Rad, Munich, Germany

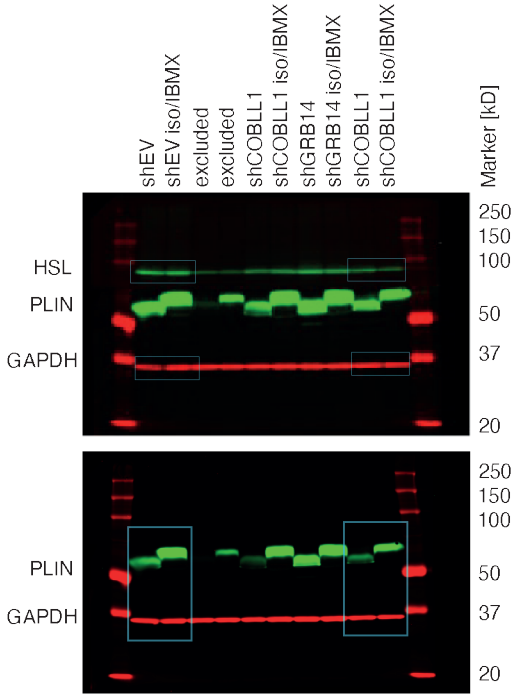

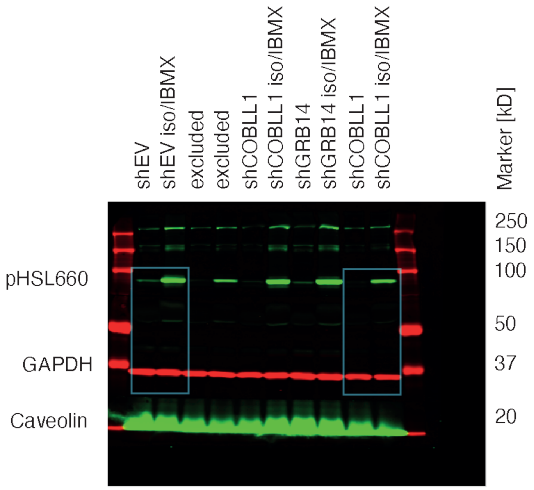

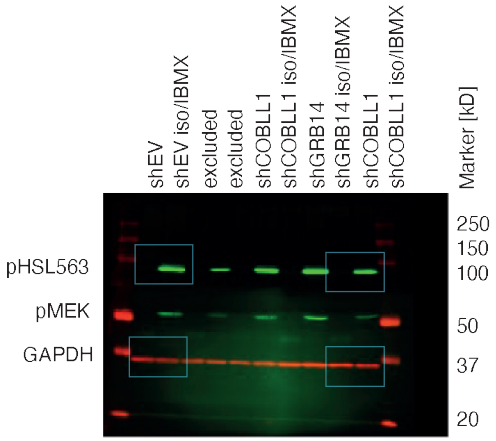

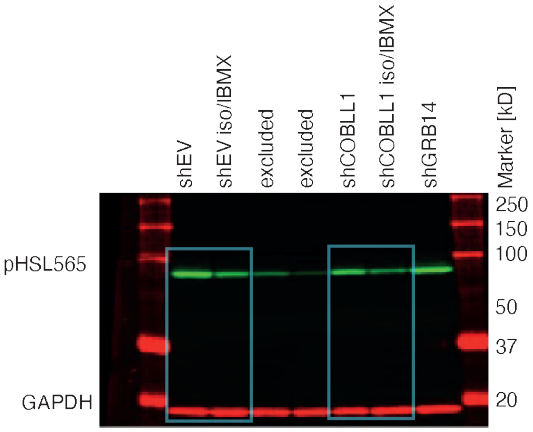

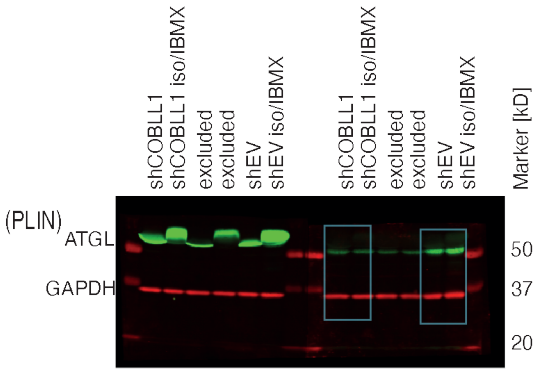

Source Data Fig. 2

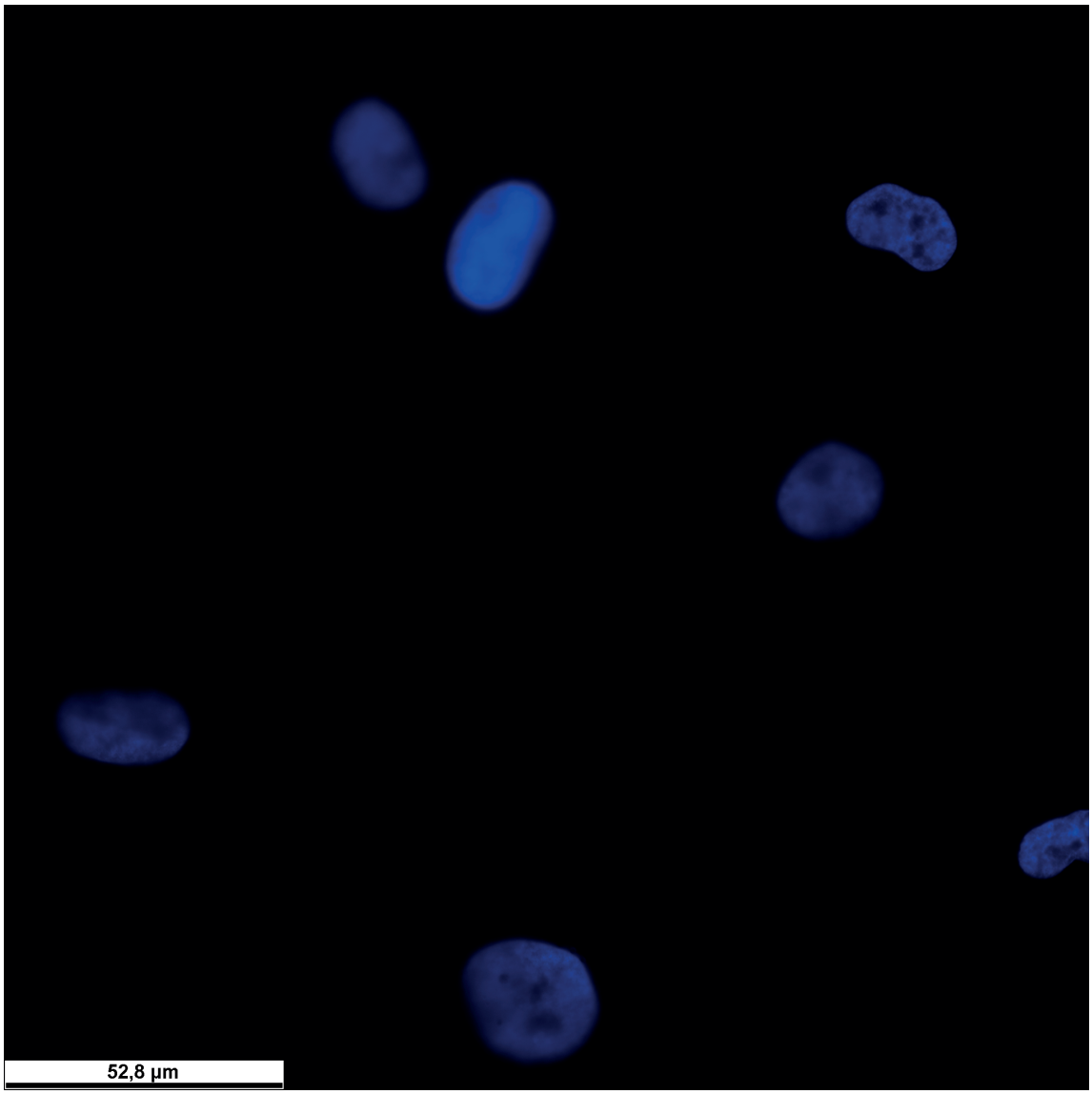

Source Data Fig. 3

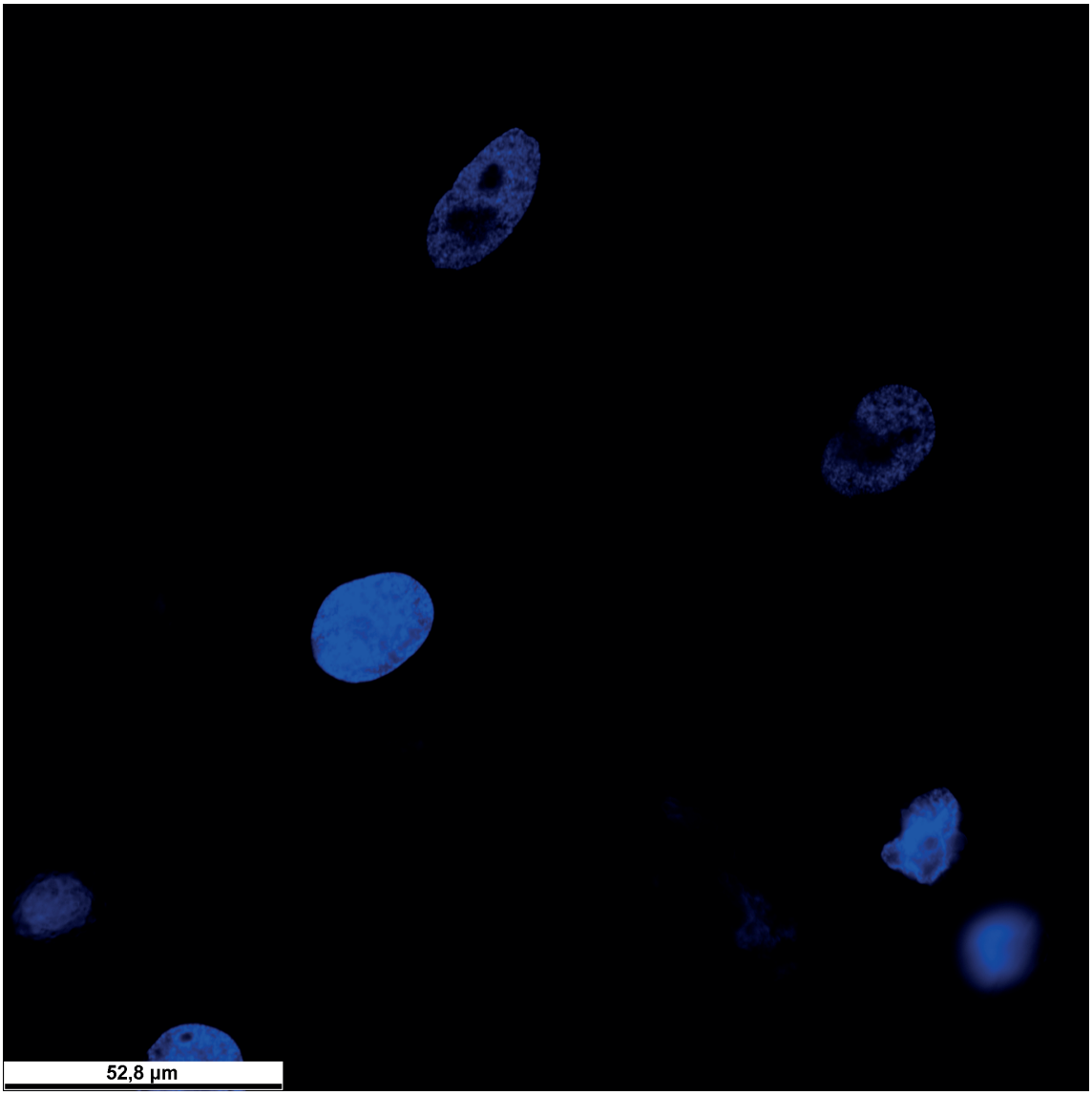

Source Data Fig. 4

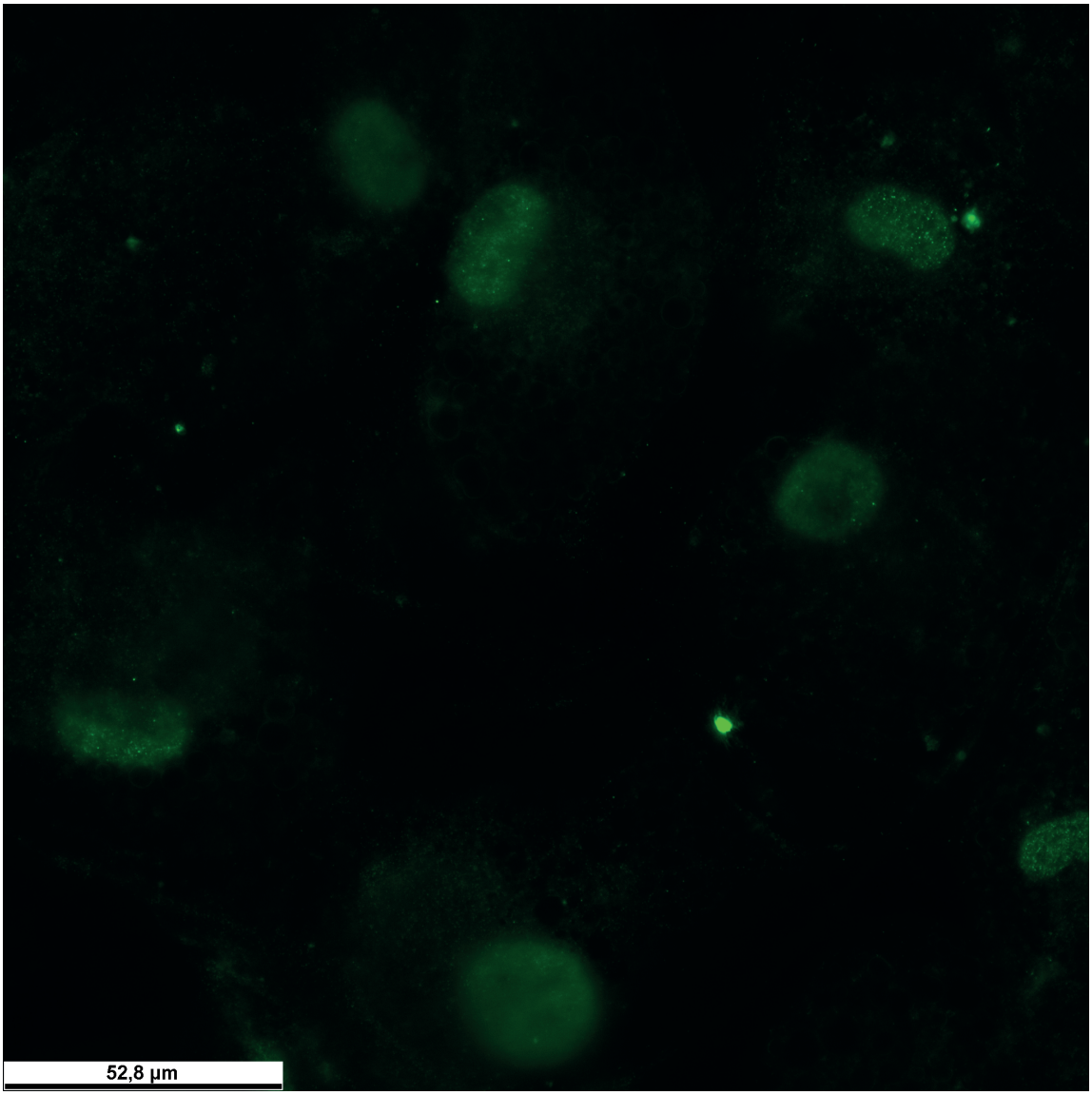

Source Data Fig. 5

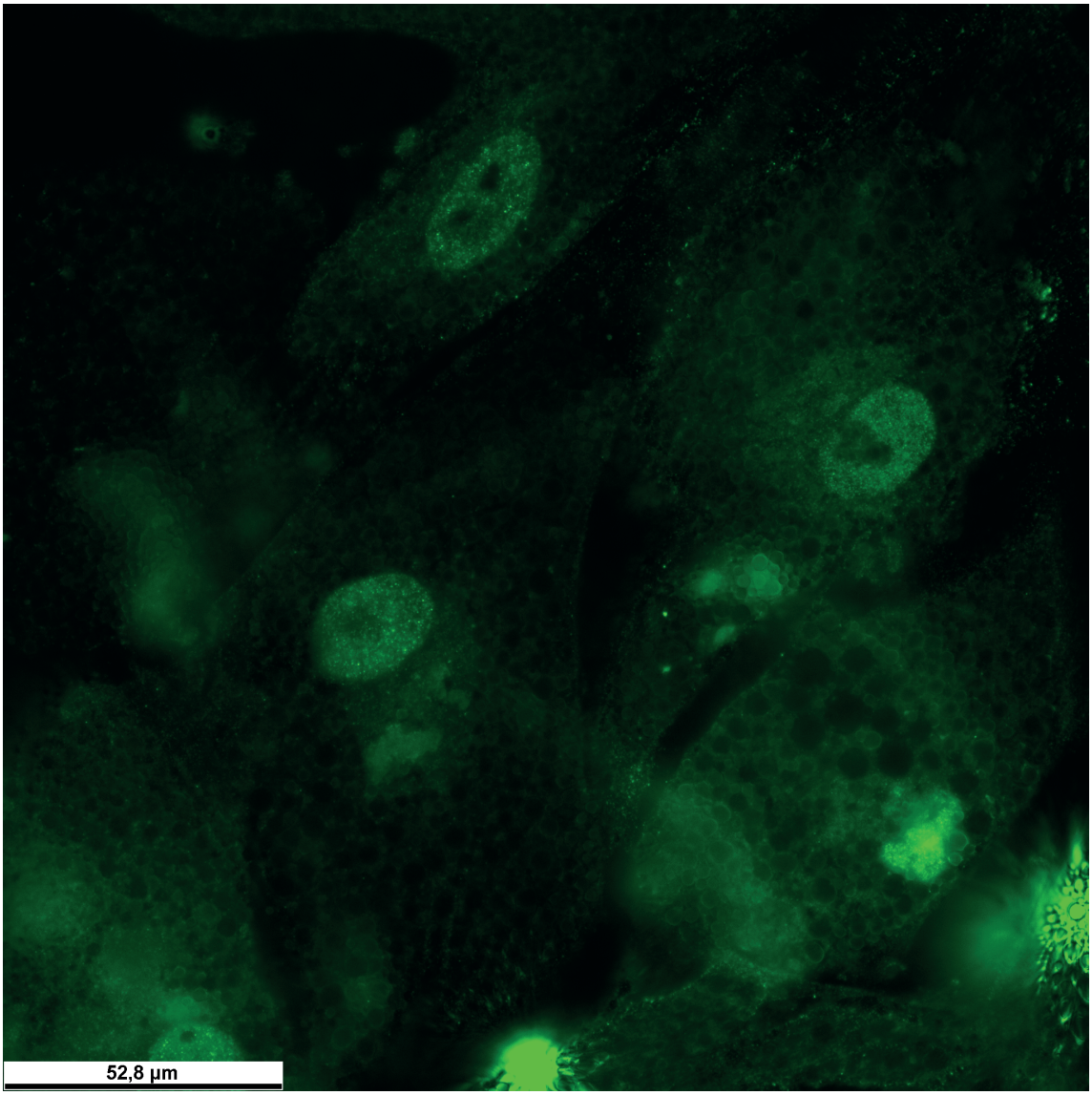

Source Data Fig. 6

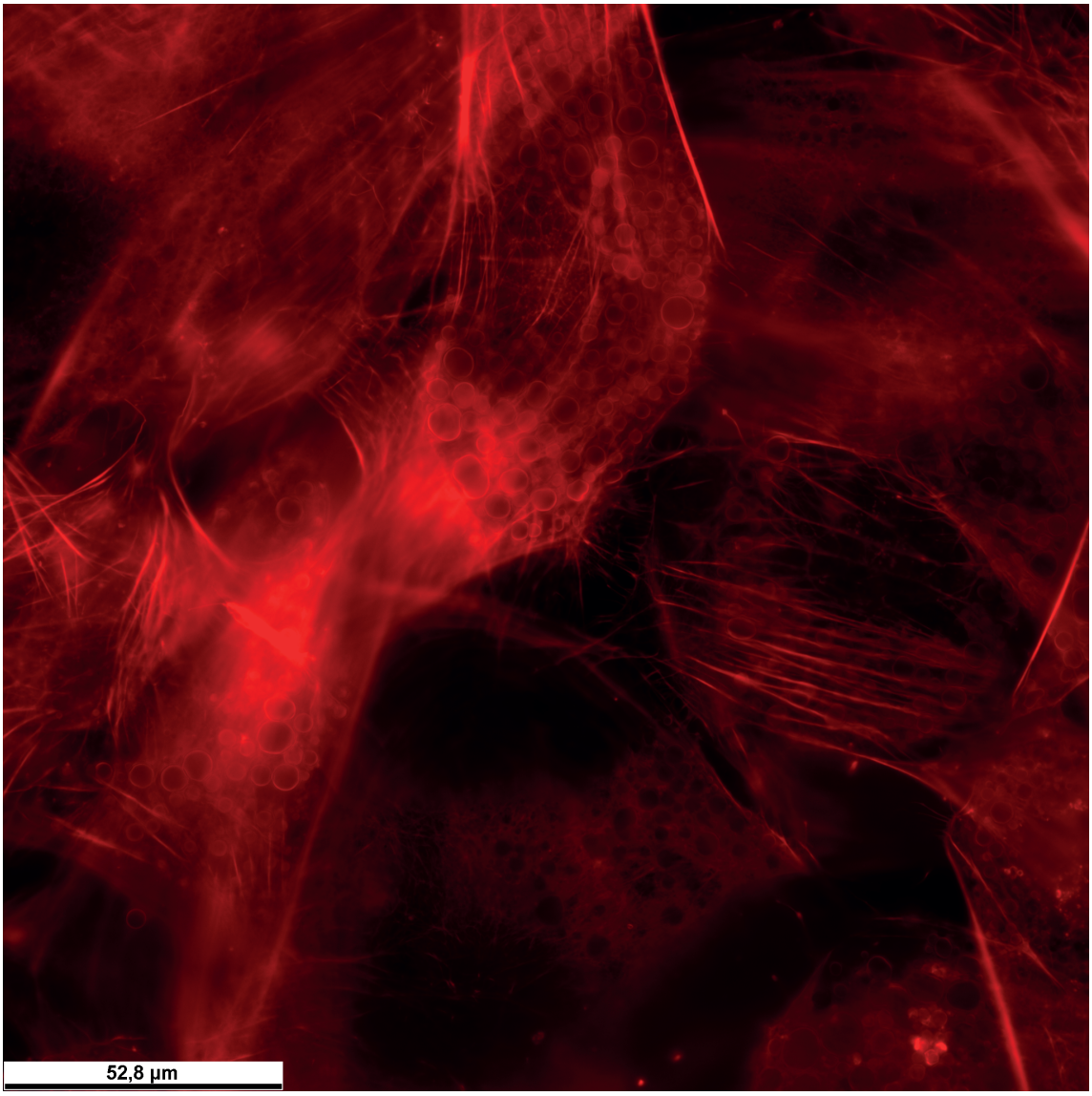

Source Data Fig. 7

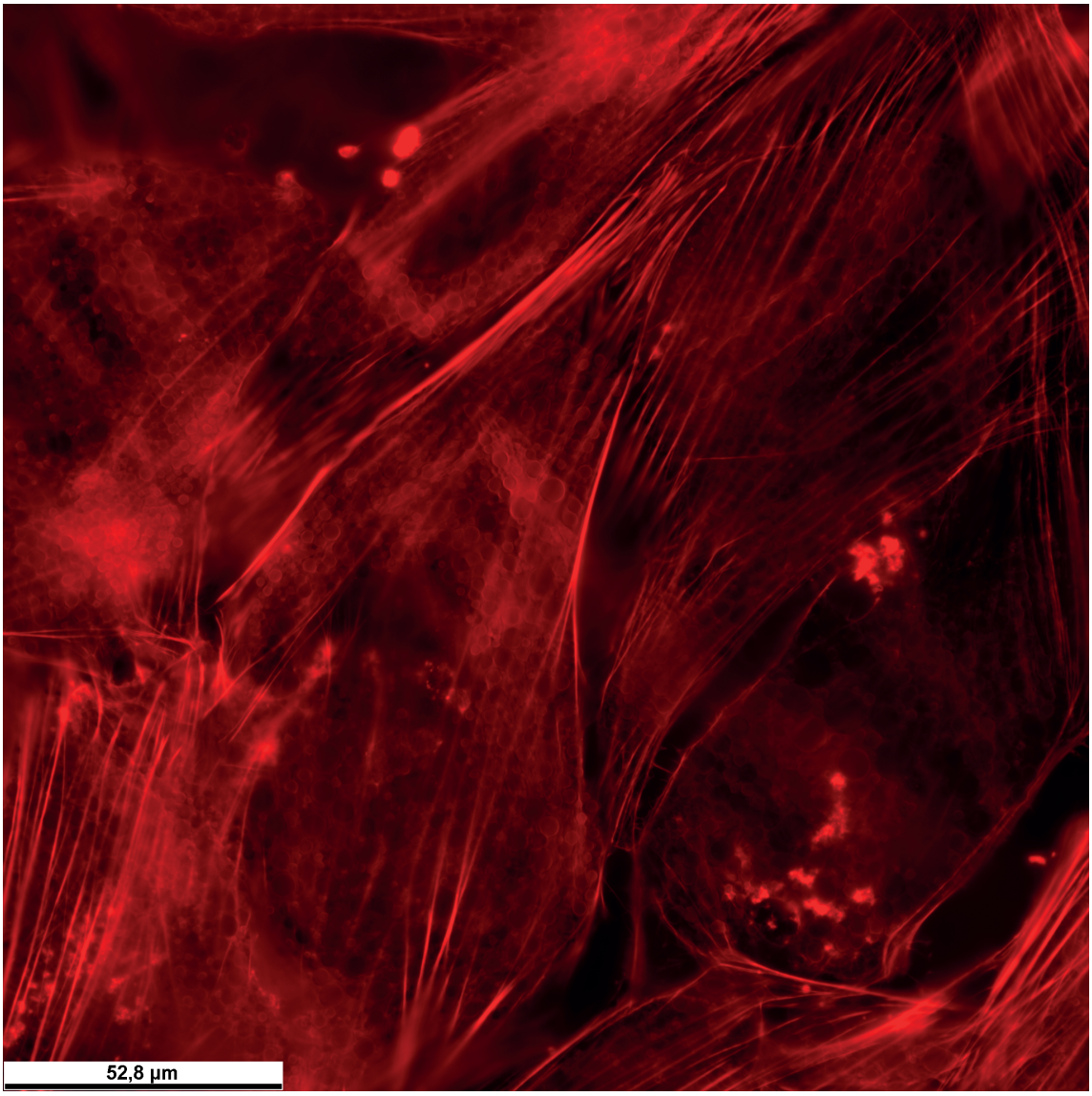

Source Data Fig. 8

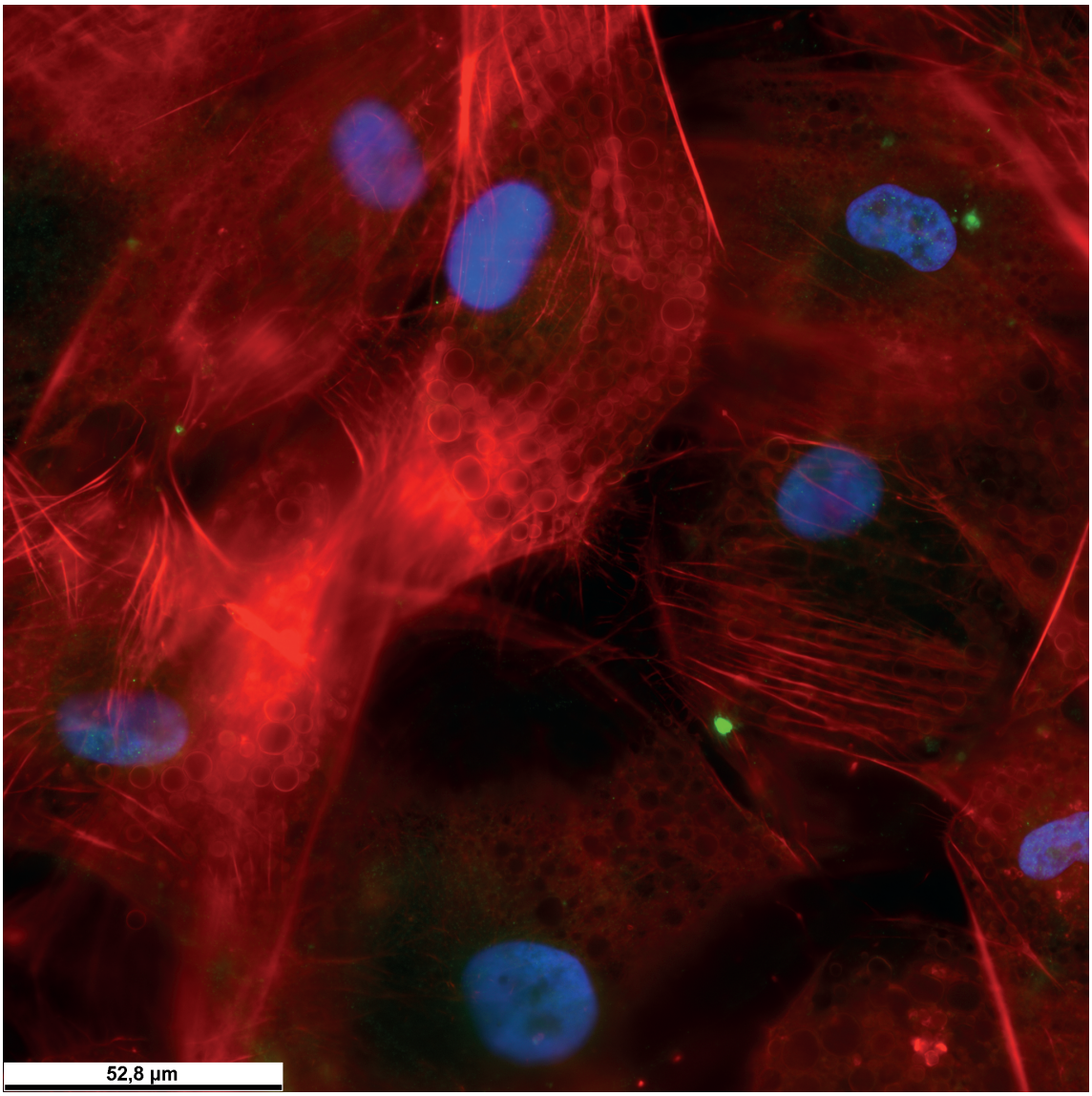

Source Data Fig. 9

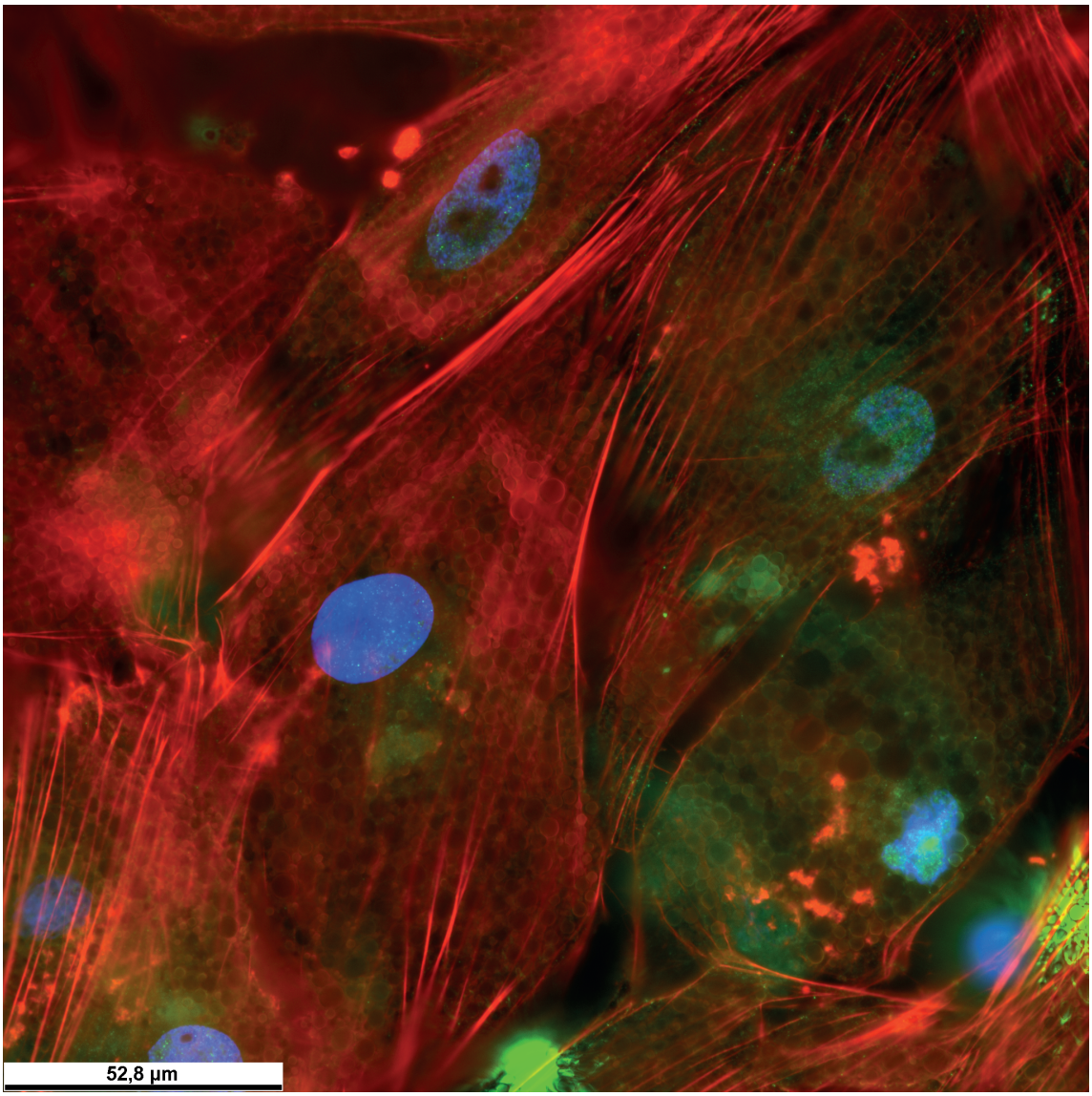

Source Data Fig. 10